

Cite this: *Dalton Trans.*, 2014, **43**, 3285

Received 31st October 2013,
Accepted 9th December 2013
DOI: 10.1039/c3dt53084a

www.rsc.org/dalton

New cobalt, iron and chromium catalysts based on easy-to-handle N_4 -chelating ligands for the coupling reaction of epoxides with CO_2 †

M. Adolph, T. A. Zevaco,* C. Altesleben, O. Walter and E. Dinjus

In this contribution, we report the successful utilization of several transition metal complexes based on substituted N_4 - N,N -bis(2-pyridinecarboxamide)-1,2-benzene chelating ligands as catalysts in the coupling of epoxides with carbon dioxide. The complexes were tested towards cyclohexene oxide and propylene oxide. Additionally the recyclability of the catalytic system was evaluated and a broader catalytic screening involving several commercially available epoxides was carried out with selected catalysts.

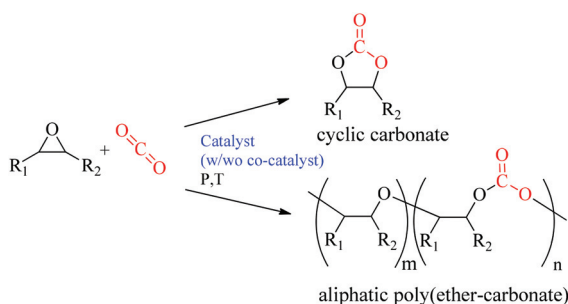
Introduction

The quest for renewable resources and sustainable systems has a foreground position in the contemporary economy and plays an ever-increasing role in different sectors of modern chemistry, as well in academia and in industry, particularly if one considers the fact that mineral oil-based resources will most probably be exhausted within the coming century. One *de facto* renewable resource of major interest is carbon dioxide. Carbon dioxide¹ is indisputably abundant, easy-to-handle, and non-toxic and is, once the problem of its thermodynamic stability is solved, an attractive raw material for organic syntheses. The coupling of epoxides (Scheme 1) with carbon dioxide which

generates cyclic carbonates – the thermodynamic products – as well as aliphatic polycarbonates – the kinetic products – is attracting growing interest from the “ CO_2 -community” mainly due to a promising range of industrial applications.² Aliphatic polycarbonates formed along this synthesis route are an important addition to the common aromatic polycarbonates owing to, amongst others, a higher intrinsic biodegradability³ (e.g. polypropylene carbonate). On the other hand, cyclic carbonates are industrially used as electrolytes in Li-ion cells, as polar, non-toxic solvents in cleaning processes or as substrates for the synthesis of high value-added molecules.⁴

Since the first catalytic system for the copolymerization of CO_2 with epoxides described by Inoue *et al.*⁵ in 1969, varieties of heterogeneous or homogeneous catalytic systems have been reported.^{6–8} These well-documented studies have in common that, in the case of homogeneous catalysts, three complementary features are required for a successful reaction: an acidic metal centre able to coordinate the epoxide, a chelating ligand with suitable geometry and a leaving group able to easily form a reactive metal–alkoxide bond. Only this bond is able to interact easily with CO_2 and keep the activation–insertion steps running. A wide range of metal/leaving group/ligand configurations has been tested and many transition metal complexes displaying these valuable characteristics were reviewed in recent years.^{9–11} Catalysts involving zinc(II), aluminum(III) and cobalt(III) seem to be currently the most promising candidates with one particular trend as far as the ligand design is concerned: the grafting of ionic moieties (ammonium or phosphonium) on the ligand backbone able to perform as co-catalysts.

Perusing the literature dealing with “renowned” chelating ligands like, e.g., *salen* (N_2O_2) investigated a.o. by Coates,¹² tetra-phenylporphyrin (N_4) pioneered by Inoue,¹³ tetramethyl-tetraazaannulene (N_4) used by Darensbourg¹⁴ and *salan* (N_2O_2),



Scheme 1 Possible products of the reaction of CO_2 with epoxides.

Institut für Katalyseforschung und -Technologie (IKFT), Karlsruher Institut für Technologie (KIT), Hermann-von-Helmholtz-Platz 1, 76344 Eggenstein-Leopoldshafen, Germany. E-mail: thomas.zevaco@kit.edu, eckhard.dinjus@kit.edu; Fax: +49 721 608-22244; Tel: +49 721 608-24385

† Electronic supplementary information (ESI) available. CCDC 958114, 958115 and 958116. For ESI and crystallographic data in CIF or other electronic format see DOI: 10.1039/c3dt53084a

salen's reduced form) by Rieger,¹⁵ some trends can be identified: on the one hand, a relatively planar geometry at the metal center guaranteed by an adequate ligand design. On the other hand, a good interplay between electron-donating/withdrawing capabilities of the ligand and Lewis acidity of the metal ion. These properties together with a good solubility of the metal complex in the epoxide-CO₂ mixture go along with the prerequisites of a copolymerization reaction. As is usual with many efficient ligand systems, the tuning of the backbone ligand should remain easy, in the same way as the up-scaling of the ligand synthesis. Additionally the tuning of the ligand framework plays a significant role in the heterogenization of the catalysts, the presence of reactive groups enabling a further grafting of an efficient homogeneous catalyst to an organic (e.g. Merrifield polymer¹⁶) or inorganic matrix¹⁷ (silica, alumina); this was revealed to be particularly interesting in the synthesis of the cyclic carbonates.

In this contribution, we report a further development of the *bpb* (*bpb*: *N,N*-bis(2-pyridinecarboxamide)-1,2-benzene) ligand system¹⁸ dealing with the variation of the diamino-linker in the ligand framework. Surprisingly, although based on a straightforward synthetic method, many derivatives are still unknown and missing in the “*bpb*-collection”. Hence we focused on new chromium, cobalt and iron complexes displaying ligand frameworks containing either electron donating groups (Me) or electron withdrawing groups (Cl and NO₂). The resulting air-stable metal complexes were thoroughly characterized and, in three cases, further investigated *via* X-ray structure determination. These complexes have been tested for the first time in catalytic screening tests involving carbon dioxide and several epoxides, mainly cyclohexene oxide and propylene oxide.

Experimental section

General procedure

All manipulations were carried out under normal atmosphere. The chemicals were of reagent grade, obtained from commercial sources such as Aldrich, abcr or Alfa Aesar and used without further purification. Cyclohexene oxide and propylene oxide were dried over CaH₂ before their use. The ligands **1–4** and the complexes **5**, **9**, **10**, **13**, **14** and **18** were synthesized according to the literature procedures reported by Yamazaki,^{19a} Vagg *et al.*,^{19b} Mukherjee *et al.*,^{20,21} Zhou *et al.*²² and Kim *et al.*²³ Compound **20** was synthesized according to our own contribution.¹⁸

The NMR spectra of the catalysts and copolymer solutions were recorded using a Varian Inova 400 spectrometer (¹H: 399.81 MHz, ¹³C: 100.54 MHz). TMS was used as an internal standard (¹³C, ¹H) with different deuterated solvents. The chemical shifts δ (in ppm) are given relative to the residual signal of the solvent. Mass spectra were measured with an Agilent 1100 MSD. Infrared spectra (KBr pellets and thin films between KBr plates) were recorded on a Varian 660-IR FT-IR Spectrometer. Molecular weights and MWD of the polymers

were measured using a Merck gel permeation chromatograph (Lichograph Gradient pump L-6200 with thermostat, LaChrom RI detector L-7490) equipped with a pre-column and two different columns (PSS SDV 5 m, 1000 and 100 Å). Toluene was used as an eluent, and calibration was performed using polystyrene standards. Elementary analysis was performed using a CHN-Analyser Vario EL III of the company Elementar. The X-ray analyses were performed using a Bruker Apex II Quazar diffractometer. Integration of the data proceeded with SAINT, the data were corrected for Lorentz- and polarisation effects, and an experimental absorption correction with SADABS was performed.²⁴ For searches relating to single-crystal X-ray diffraction data, the Cambridge Structural Database was used.²⁵ Figures were prepared with the appropriate software of the CCDC, MERCURY 3.0 (Build RC5) for Windows.²⁶ Crystallographic data of the structures have been deposited at the Cambridge Crystallographic Database Centre, supplementary publication no.: CCDC 958116 for complex **23** (LMe₂), 958114 for complex **6** (LCl₂) and 958115 for **22** (LNO₂).

Synthesis of 6–8. 2.0 mmol of CoOAc₂·4H₂O and 2.0 mmol of the appropriate ligand (**2–4**) were dissolved in 15 ml of DMF and stirred at RT under air for 10 min. Then 2.88 mmol of NEt₄OAc·4H₂O were added and the solution was stirred at 70 °C for 12 h. After cooling, the solution was stirred for an additional 6 hours. DMF was removed *in vacuo* and the residue was dissolved in 20 ml of acetonitrile. A precipitate was formed on adding 20 ml of diethyl ether to the solution and cooling down to 2 °C. The product was isolated after filtering, washing two times with 20 ml of a 1 : 1 acetonitrile–diethyl ether mixture and drying under vacuum. For complex **6** green crystals were obtained by slowly adding a small excess of diethyl ether into an acetonitrile solution of **5** and subsequently cooling down to 2 °C. After 2 days small green crystals were formed.

6: green powder/crystals, Yield: 78%. IR (cm^{−1}): 2985 (w), 2924 (w), 2853 (w), 1625 (s), 1598 (s), 1557 (m), 1470 (s), 1400 (m), 1314 (m), 1229 (w), 1102 (w), 1002 (w), 977 (w), 926 (w), 764 (w), 683 (m), 670 (m), 548 (w). ¹H-NMR δ (ppm, dmsd-d₆) = 1.01 (s, 6 H), 1.10 (t, *J* = 7.3 Hz, 12 H), 3.15 (q, *J* = 7.3 Hz, 8 H), 7.65–7.69 (m, 2 H), 7.84 (dd, *J* = 7.6 Hz, *J* = 1.5 Hz, 2 H), 8.07 (t, *J* = 7.3 Hz, 2 H), 8.88 (d, *J* = 0.6 Hz, 2 H), 10.09 (d, *J* = 5.8 Hz, 2 H). ¹³C{¹H}NMR/DEPT135 (prim. = primary carbon; sec. = secondary carbon; tert. = tertiary carbon; quat. = quaternary carbon): δ (ppm, dmsd-d₆) = 7.1 (prim., 4 C), 24.1 (prim., 2 C), 51.4 (sec., 4 C), 121.0 (tert., 2 C), 122.5 (tert., 2 C; quat., 2 C), 124.3 (tert., 2 C), 139.5 (tert., 2 C), 143.7 (quat., 2 C), 156.8 (tert., 2 C), 158.8 (quat., 2 C), 166.5 (quat., 2 C), 175.9 (quat., 2 C). MS: (ESI[−]) *m/z* = 561 [M − NEt₄][−]. Anal. Calcd for C₃₀H₃₆Cl₂CoN₅O₆: C, 52.03; H, 5.24; N, 10.11. Found: C, 51.27; H, 5.49; N, 10.05.

7: brown powder, Yield: 63%. IR (cm^{−1}): 3081 (w), 2985 (w), 2926 (w), 1629 (vs), 1601 (s), 1557 (m), 1482 (s), 1427 (m), 1386 (s), 1315 (vs), 1297 (s), 1146 (m), 1062 (w), 1002 (w), 957 (w), 898 (w), 756 (w), 683 (m), 616 (m), 505 (w), 464 (w). ¹H-NMR δ (ppm, CD₃CN) = 1.01 (s, 6 H), 1.09 (tt, *J* = 7.3 Hz, *J* = 1.7 Hz, 12 H), 3.13 (q, *J* = 7.2 Hz, 8 H), 7.65–7.73 (m, 2 H), 7.88

(dt, $J = 8.6$ Hz, $J = 1.6$ Hz, 3 H), 8.06–8.12 (m, 2 H), 8.82 (d, $J = 9.0$ Hz, 1 H), 9.54 (d, $J = 2.6$ Hz, 2 H), 10.10 (dd, $J = 12.2$ Hz, $J = 5.3$ Hz, 2 H). $^{13}\text{C}\{^1\text{H}\}$ -NMR/DEPT135: δ (ppm, CD_3CN) = 7.5 (prim., 4 C), 24.5 (prim., 2 C), 51.8 (sec., 4 C), 116.0 (tert., 1 C), 119.5 (tert., 1 C), 120.1 (tert., 1 C), 123.0 (tert., 1 C), 123.3 (tert., 1 C), 124.8 (tert., 1 C), 125.1 (tert., 1 C), 140.0 (tert., 2 C), 141.8 (quat., 1 C), 144.2 (quat., 1 C), 151.3 (quat., 1 C), 157.1 (tert., 1 C), 157.2 (tert., 1 C), 158.7 (quat., 1 C), 159.2 (quat., 1 C), 167.2 (quat., 1 C), 167.7 (quat., 1 C), 176.4 (quat., 2 C). MS: (ESI $^-$) m/z = 538 $[\text{M} - \text{NEt}_4]^+$. Anal. Calcd for $\text{C}_{30}\text{H}_{37}\text{CoN}_6\text{O}_8\cdot\text{H}_2\text{O}$: C, 53.89; H, 5.73; N, 12.24. Found: C, 52.48; H, 5.72; N, 12.49.

8: green powder, Yield: 51%. IR (cm^{-1}): 3087 (w), 2978 (w), 2921 (w), 2857 (w), 1621 (s), 1596 (vs), 1485 (s), 1456 (m), 1405 (s), 1371 (s), 1316 (m), 1172 (w), 1095 (w), 1001 (m), 886 (w), 759 (m), 681 (m), 619 (w), 509 (w). ^1H -NMR δ (ppm, $\text{dmsO}-d_6$) = 1.02 (s, 6 H), 1.15 (t, $J = 7.3$ Hz, 12 H), 2.24 (s, 6 H), 3.20 (q, $J = 7.2$ Hz, 8 H), 7.64 (ddd, $J = 7.4$ Hz, $J = 5.6$ Hz, $J = 1.6$ Hz, 2 H), 7.83 (dd, $J = 7.7$ Hz, $J = 1.2$ Hz, 2 H), 8.07 (dt, $J = 7.6$ Hz, $J = 1.3$ Hz, 2 H), 8.62 (s, 2 H), 10.16 (d, $J = 5.5$ Hz, 2 H). $^{13}\text{C}\{^1\text{H}\}$ -NMR/DEPT135: δ (ppm, $\text{dmsO}-d_6$) = 7.1 (prim., 4 C), 19.8 (prim., 2 C), 24.2 (prim., 2 C), 51.4 (sec., 4 C), 122.1 (tert., 2 C), 122.4 (tert., 2 C), 123.5 (tert., 2 C), 129.5 (quat., 2 C), 139.1 (quat., 2 C), 141.7 (tert., 2 C), 156.8 (quat., 2 C), 160.2 (tert., 2 C), 165.3 (quat., 2 C), 175.8 (quat., 2 C). MS: (ESI $^-$) m/z = 521 $[\text{M} - \text{NEt}_4]^+$. Anal. Calcd for $\text{C}_{32}\text{H}_{42}\text{CoN}_5\text{O}_6\cdot\text{H}_2\text{O}$: C, 57.39; H, 6.62; N, 10.46. Found: C, 56.22; H, 6.89; N, 10.34.

Synthesis of 11 and 12. 2.0 mmol of CoCl_2 , 2.0 mmol of the corresponding ligand (3–4), 4.0 mmol of triethylamine and 4.42 mmol of $\text{NEt}_4\text{Cl}\cdot\text{H}_2\text{O}$ were dissolved in 15 ml of DMF and stirred at RT under normal atmosphere for 12 hours. DMF was removed *in vacuo* and 50 ml of acetonitrile was added to the residue. A precipitate was formed, which was filtered and washed with 20 ml of a 1:1 acetonitrile–diethyl ether mixture. After drying under vacuum the product was isolated.

11: red-brown powder/crystals, Yield: 91%. IR (cm^{-1}): 3070 (w), 2986 (w), 2949 (w), 1632 (vs), 1600 (s), 1558 (s), 1481 (vs), 1426 (m), 1390 (s), 1319 (vs), 1296 (s), 1142 (m), 1062 (m), 999 (w), 958 (w), 895 (w), 758 (m), 684 (m), 615 (w), 508 (w), 465 (w), 352 (w). ^1H -NMR δ (ppm, CD_3CN) = 1.12–1.19 (m, 12 H), 3.11 (q, $J = 7.3$ Hz, 8 H), 7.80–7.86 (m, 2 H), 7.94 (dd, $J = 9.0$ Hz, $J = 2.6$ Hz, 1 H), 8.10–8.21 (m, 4 H), 8.93 (d, $J = 8.8$ Hz, 1 H), 9.60–9.67 (m, 3 H). $^{13}\text{C}\{^1\text{H}\}$ -NMR/DEPT135: δ (ppm, CD_3CN) = 7.5 (prim., 4 C), 52.9 (sec., 4 C), 117.5 (tert., 1 C), 120.4 (tert., 1 C), 121.4 (tert., 1 C), 125.0 (tert., 1 C), 125.3 (tert., 1 C), 128.4 (tert., 1 C), 128.7 (tert., 1 C), 140.5 (tert., 2 C), 143.5 (quat., 1 C), 144.3 (quat., 1 C), 151.0 (quat., 1 C), 152.0 (tert., 1 C), 152.1 (tert., 1 C), 160.5 (quat., 1 C), 161.0 (quat., 1 C), 168.0 (quat., 1 C), 168.4 (quat., 1 C). MS: (ESI $^-$) m/z = 490 $[\text{M} - \text{NEt}_4]^+$. Anal. Calcd for $\text{C}_{26}\text{H}_{31}\text{Cl}_2\text{CoN}_6\text{O}_4$: C, 50.25; H, 5.03; N, 13.52. Found: C, 50.05; H, 4.96; N, 13.67.

12: red powder, Yield: 88%. IR (cm^{-1}): 3077 (w), 2984 (w), 2924 (w), 2856 (w), 1625 (vs), 1595 (s), 1577 (s), 1486 (m), 1456 (m), 1404 (s), 1290 (m), 1251 (m), 1178 (m), 1092 (w),

1003 (w), 943 (w), 889 (w), 765 (m), 681 (m), 651 (w), 509 (w), 406 (w). ^1H -NMR δ (ppm, CD_3CN) = 1.16 (t, $J = 7.3$ Hz, 12 H), 2.29 (s, 6 H), 3.10 (q, $J = 7.3$ Hz, 8 H), 7.76 (t, $J = 6.4$ Hz, 2 H), 8.05–8.16 (m, 4 H), 8.68 (s, 2 H), 9.64 (d, $J = 5.5$ Hz, 2 H). $^{13}\text{C}\{^1\text{H}\}$ -NMR/DEPT135: δ (ppm, CD_3CN) = 7.6 (prim., 4 C), 20.0 (prim., 2 C), 52.9 (sec., 4 C), 123.9 (tert., 2 C), 124.4 (tert., 2 C), 127.5 (tert., 2 C), 131.9 (quat., 2 C), 140.0 (tert., 2 C), 142.1 (quat., 2 C), 151.7 (tert., 2 C), 162.4 (quat., 2 C). MS: (ESI $^-$) m/z = 473 $[\text{M} - \text{NEt}_4]^+$. Anal. Calcd for $\text{C}_{28}\text{H}_{36}\text{Cl}_2\text{CoN}_5\text{O}_2\cdot\text{H}_2\text{O}$: C, 54.03; H, 6.15; N, 11.25. Found: C, 54.26; H, 6.39; N, 11.38.

Synthesis of 15 and 16. 2.0 mmol of FeCl_3 , 2.0 mmol of the corresponding ligand (3–4), 4.0 mmol of triethylamine and 4.42 mmol of $\text{NEt}_4\text{Cl}\cdot\text{H}_2\text{O}$ were dissolved in 15 ml of DMF and stirred at RT under air for 12 hours. DMF was removed *in vacuo* and 50 ml of acetonitrile for 15 and for 16 20 ml of a 1:1 acetonitrile–diethyl ether mixture were added to the residue. The resulting precipitate was filtered and washed twice (for 16 thrice) with 20 ml of a 1:1 acetonitrile–diethyl ether mixture and eventually dried under vacuum.

15: green powder, Yield: 80%. IR (cm^{-1}): 3122 (w), 3068 (w), 2983 (w), 2925 (w), 1625 (vs), 1594 (s), 1559 (s), 1506 (m), 1471 (m), 1421 (w), 1346 (s), 1323 (vs), 1296 (s), 1136 (m), 1113 (m), 1045 (w), 1000 (w), 969 (w), 924 (w), 827 (w), 760 (m), 696 (m), 647 (w), 488 (m). MS: (ESI $^-$) m/z = 487 (100%), 489 (65%) $[\text{M} - \text{NEt}_4]^+$. Anal. Calcd for $\text{C}_{26}\text{H}_{31}\text{Cl}_2\text{FeN}_6\text{O}_4\cdot\text{H}_2\text{O}$: C, 49.08; H, 5.23; N, 13.21. Found: C, 49.18; H, 4.95; N, 13.40.

16: dark-green powder, Yield: 68%. IR (cm^{-1}): 3045 (w), 2985 (w), 2915 (w), 2865 (w), 1615 (s), 1582 (vs), 1563 (s), 1478 (s), 1455 (m), 1401 (m), 1354 (s), 1287 (m), 1254 (w), 1182 (w), 1093 (w), 1044 (m), 1002 (w), 954 (w), 893 (w), 764 (m), 695 (m), 648 (w), 504 (w), 470 (w). MS: (ESI $^-$) m/z = 470 $[\text{M} - \text{NEt}_4]^+$. Anal. Calcd for $\text{C}_{28}\text{H}_{36}\text{Cl}_2\text{FeN}_5\text{O}_2\cdot 2\text{H}_2\text{O}$: C, 52.76; H, 6.33; N, 10.99. Found: C, 53.03; H, 6.62; N, 11.19.

Synthesis of 17 and 19. 2.0 mmol of $\text{CrCl}_3\cdot 6\text{H}_2\text{O}$, 2.0 mmol of the ligand (1 or 4), 4.0 mmol of triethylamine and 4.42 mmol of $\text{NEt}_4\text{Cl}\cdot\text{H}_2\text{O}$ were dissolved in 15 ml of DMF and stirred at 120 °C for 12 hours. After cooling the solution was stirred at RT and under air for an additional 6 hours. DMF was removed *in vacuo* and 20 ml of a 1:1 acetonitrile–diethyl ether mixture was added to the residue yielding a precipitate, which was filtered, washed twice with 20 ml of a 1:1 acetonitrile–diethyl ether mixture and dried under vacuum.

17: red powder, Yield: 88%. IR (cm^{-1}): 3055 (w), 2987 (w), 2946 (w), 1620 (s), 1592 (vs), 1565 (vs), 1471 (s), 1363 (s), 1289 (m), 1183 (w), 1146 (w), 1094 (w), 1036 (m), 961 (w), 906 (w), 764 (m), 690 (m), 654 (w), 595 (w), 511 (m), 328 (m). MS: (ESI $^-$) m/z = 438 $[\text{M} - \text{NEt}_4]^+$. Anal. Calcd for $\text{C}_{26}\text{H}_{32}\text{Cl}_2\text{CrN}_5\text{O}_2\cdot\text{H}_2\text{O}$: C, 53.16; H, 5.83; N, 11.92. Found: C, 52.48; H, 5.57; N, 11.86.

19: red-brown powder, Yield: 87%. IR (cm^{-1}): 3067 (w), 2981 (w), 2924 (w), 1629 (s), 1562 (vs), 1514 (m), 1482 (s), 1366 (s), 1291 (m), 1238 (w), 1178 (m), 1095 (w), 1048 (w), 1003 (w), 892 (w), 764 (w), 695 (m), 663 (w), 510 (w), 422 (w). MS: (ESI $^-$) m/z = 466 $[\text{M} - \text{NEt}_4]^+$. Anal. Calcd for $\text{C}_{28}\text{H}_{36}\text{Cl}_2\text{CrN}_5\text{O}_2\cdot 2\text{H}_2\text{O}$: C, 53.08; H, 6.36; N, 11.05. Found: C, 52.76; H, 6.33; N, 11.42.

Synthesis of 21–23. 2.0 mmol of $\text{CoBr}_2 \cdot x\text{H}_2\text{O}$, 2.0 mmol of the related ligand (2–4), 4.0 mmol of triethylamine and 4.42 mmol of NEt_4Br were dissolved in 15 ml of DMF and stirred under air at RT for 12 hours. DMF was removed *in vacuo* and 50 ml of acetonitrile (for 21 20 ml) was added to the residue. A precipitate was formed, which was filtered and washed twice (for 17 thrice) with 20 ml of a 1 : 1 acetonitrile–diethyl ether mixture. After drying under vacuum the product was obtained. For complex 22 red-brown crystals were obtained by slowly adding a small excess of diethyl ether into an acetonitrile solution of 22 and subsequently cooling down to 2 °C. After 2 days small red-brown crystals were formed. Using the same procedure brown crystals for 23 could be isolated.

21: brown powder, Yield: 65%. IR (cm^{-1}): 3086 (w), 3051 (w), 2982 (w), 2945 (w), 1626 (vs), 1598 (s), 1558 (s), 1468 (s), 1395 (s), 1285 (m), 1200 (w), 1097 (m), 1049 (w), 975 (m), 925 (w), 887 (w), 760 (m), 680 (m), 546 (m), 482 (w), 447 (w). $^1\text{H-NMR}$ δ (ppm, CD_3CN) = 1.18 (t, J = 7.2 Hz, 12 H), 3.13 (q, J = 7.2 Hz, 8 H), 7.83 (tr, J = 6.3 Hz, 2 H), 8.07–8.17 (m, 4 H), 9.00 (s, 2 H), 9.70 (d, J = 5.3 Hz, 2 H). $^{13}\text{C}\{^1\text{H}\}$ -NMR/DEPT135: δ (ppm, CD_3CN) = 7.6 (prim., 4 C), 52.9 (sec., 4 C), 123.3 (tert., 2 C), 124.9 (tert., 2 C), 125.1 (quat., 2 C), 128.4 (tert., 2 C), 140.3 (tert., 2 C), 144.1 (quat., 2 C), 153.0 (tert., 2 C), 161.6 (quat., 2 C), 167.9 (quat., 2 C). MS: (ESI $^-$) m/z = 602 [$\text{M} - \text{NEt}_4$] $^-$. Anal. Calcd for $\text{C}_{26}\text{H}_{30}\text{Br}_2\text{Cl}_2\text{CoN}_5\text{O}_2$: C, 42.53; H, 4.12; N, 9.54. Found: C, 42.08; H, 4.52; N, 10.12.

22: red-brown powder/crystals, Yield: 62%. IR (cm^{-1}): 3124 (w), 3054 (w), 2987 (w), 2925 (w), 1631 (vs), 1598 (s), 1558 (vs), 1493 (s), 1478 (s), 1422 (m), 1389 (s), 1318 (s), 1293 (s), 1140 (m), 1094 (w), 1058 (m), 998 (w), 985 (w), 897 (w), 759 (m), 682 (m), 616 (w), 506 (w), 459 (w). $^1\text{H-NMR}$ δ (ppm, CD_3CN) = 1.15–1.21 (m, 12 H), 3.14 (q, J = 7.2 Hz, 8 H), 7.83–7.90 (m, 2 H), 7.95 (dd, J = 8.9 Hz, J = 2.5 Hz, 1 H), 8.14–8.20 (m, 4 H), 8.96 (d, J = 9.0 Hz, 1 H), 9.65–9.74 (m, 3 H). $^{13}\text{C}\{^1\text{H}\}$ -NMR/DEPT135: δ (ppm, CD_3CN) = 7.6 (prim., 4 C), 52.9 (sec., 4 C), 117.9 (tert., 1 C), 120.5 (tert., 1 C), 121.8 (tert., 1 C), 125.0 (tert., 1 C), 125.3 (tert., 1 C), 128.5 (tert., 1 C), 128.8 (tert., 1 C), 140.4 (tert., 1 C), 140.5 (tert., 1 C), 143.6 (quat., 1 C), 143.7 (quat., 1 C), 151.1 (quat., 1 C), 153.0 (tert., 1 C), 153.1 (tert., 1 C), 161.2 (quat., 1 C), 161.7 (quat., 1 C), 167.5 (quat., 1 C), 167.7 (quat., 1 C). MS: (ESI $^-$) m/z = 580 [$\text{M} - \text{NEt}_4$] $^-$. Anal. Calcd for $\text{C}_{26}\text{H}_{31}\text{Br}_2\text{CoN}_6\text{O}_4$: C, 43.96; H, 4.40; N, 11.83. Found: C, 43.68; H, 4.41; N, 12.25.

23: brown powder/crystals, Yield: 74%. IR (cm^{-1}): 3077 (w), 2984 (w), 2923 (w), 2858 (w), 1625 (s), 1594 (vs), 1485 (s), 1456 (m), 1404 (s), 1290 (w), 1251 (w), 1178 (w), 1093 (w), 1003 (m), 889 (w), 764 (m), 680 (m), 588 (w), 509 (w), 406 (w). $^1\text{H-NMR}$ δ (ppm, CD_3CN) = 1.15–1.20 (m, 12 H), 2.29 (s, 6 H), 3.13 (q, J = 7.3 Hz, 8 H), 7.72–7.90 (m, 2H), 8.02–8.28 (m, 4 H), 8.68 (s, 2 H), 9.56–9.70 (m, 2 H). $^{13}\text{C}\{^1\text{H}\}$ -NMR/DEPT135: δ (ppm, CD_3CN) = 7.6 (prim., 4 C), 20.0 (prim., 2 C), 53.0 (sec., 4 C), 124.3 (tert., 2 C), 124.4 (tert., 2 C), 127.7 (tert., 2 C), 127.7 (quat., 2 C), 132.2 (quat., 2 C), 140.0 (tert., 2 C), 142.0 (quat., 2 C), 152.7 (tert., 2 C), 163.1 (quat., 2 C). MS: (ESI $^-$) m/z = 561 [$\text{M} - \text{NEt}_4$] $^-$. Anal. Calcd for $\text{C}_{28}\text{H}_{36}\text{CoN}_5\text{O}_2 \cdot \text{H}_2\text{O}$: C, 47.27; H, 5.38; N, 9.84. Found: C, 46.28; H, 5.34; N, 9.71.

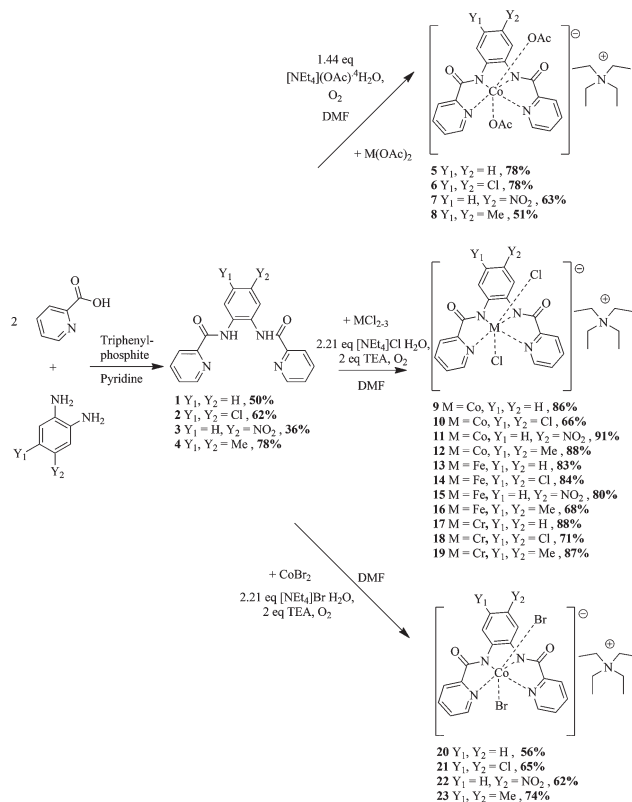
Autoclave experiments

The copolymerization tests were conducted in a screening test-bench consisting of eight 70 ml autoclaves (material 1.4571-stainless austenitic steel-316Ti, 70 ml, P_{max} 200 bar, T_{max} 250 °C) equipped with magnetic stirring and P,T-acquisition *via* multi-meters (Agilent 34970A Data Acquisition/Data Logger Switch Unit + 34901A 20 Channel Multiplexer) and PCs. The heating was performed with an aluminum heating block controlled *via* the electronic contact thermometer of the magnetic stirrers. Each configuration reported in the “reactivity” tables (4, 5 and 6) is tested two times and, if needed, a third time; the reproducibility was high. The autoclaves were dried at 110 °C under vacuum for a couple of hours, cooled down and purged with argon before use. This procedure was once again applied for two hours at 60 °C with the sole catalyst in the autoclave. After cooling the autoclave to room temperature, the epoxide was injected under argon *via* one of the autoclave ports and the reaction mixture was pressurized with CO_2 . After the reaction the autoclaves were cooled down, slowly vented under stirring in a fume hood, opened and the remaining solution (resp. solid) was collected with dichloromethane. After thorough drying, the solution (resp. solid) was firstly investigated *via* IR and $^1\text{H-NMR}$ -spectroscopy given that cyclic monomers and polycarbonates are easily differentiated *via* both spectroscopy methods. For instance, the stretching mode²⁷ of the $\text{C}=\text{O}$ bond in polycarbonates can be found at around 1750 cm^{-1} whereas the cyclic carbonates are typically found at around 1800 (*cis*-cyclohexylene carbonate at 1802 cm^{-1} , *trans*-cyclohexylene carbonate at 1818 cm^{-1} and propylene carbonate at 1800 cm^{-1}). If the solution contains a copolymer, which was the case only for cyclohexene oxide, it was next dissolved in a small amount of CH_2Cl_2 and the copolymer was precipitated utilizing 1M HCl/MeOH according to the literature.²⁸ The isolated copolymers were dried under vacuum and analyzed *via* $^1\text{H-NMR}$ spectroscopy (% carbonate linkages²⁹), $^{13}\text{C-NMR}$ -spectroscopy (tacticity) and gel permeation chromatography (molecular weights and polydispersity indexes). However, if only the cyclic monomer was obtained, the effective cyclic carbonate amount was calculated by subtracting the amount of catalyst used.

Results and discussion

Synthetic procedures

The synthesis of the bpb-metal complexes is shown in Scheme 2. The different bpb ligands (1–4) are obtained by condensation of 1,2-diaminobenzene with two equivalents of 2-pyridine-carboxylic acid in pyridine under activation with triphenyl phosphite according to Yamazaki^{19a} and Vagg.^{19b} The bpb-metal complexes are formed in a following step *via* reaction of the different ligands with one equivalent of the hydrated metal salts (MX_2 for $\text{M} = \text{Co}$, $\text{X} = \text{OAc}$, Cl , Br and MX_3 for $\text{M} = \text{Fe}$, Cr , $\text{X} = \text{Cl}$) and a slight excess of a tetraethyl ammonium salt [NEt_4] $\text{X} \cdot \text{H}_2\text{O}$ ($\text{X} = \text{OAc}$, Cl and Br) in DMF. In the case of the metal halides two equivalents of triethylamine



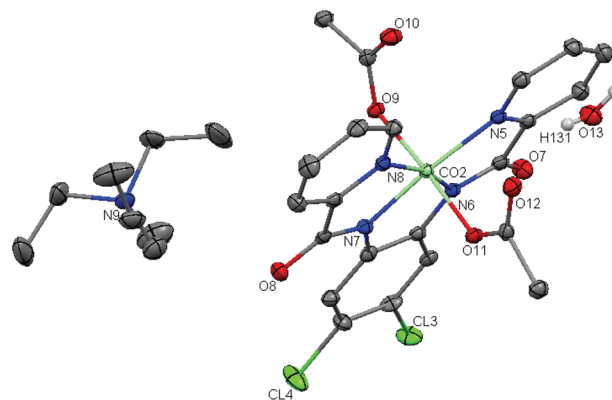
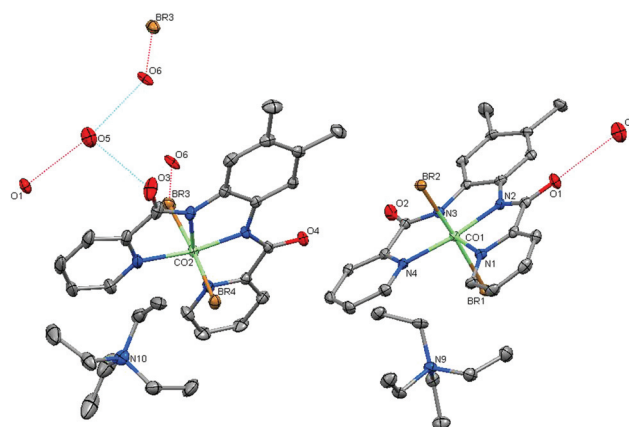
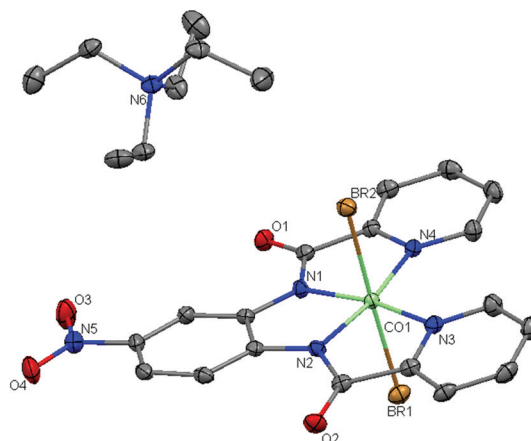
Scheme 2 Synthesis of the bpb-metal complexes.

are required for the deprotonation of the ligand's N-H, whereas using cobalt acetate, no additional base is required. The formation of the bpb complexes is generally straightforward and, for some of the complexes, a literature-known procedure (see the Experimental section for details). However, the synthesis of a chromium bpb-complex with a nitro-substituent was revealed to be more complicated than expected, yielding complex mixtures.

The new complexes **6–8**, **11**, **12**, **15–17**, **19**, and **21–23** were also characterized *via* NMR-spectroscopy, elemental analysis, IR-spectroscopy and MS-ESI, the analytic data being in good agreement with the values found in the literature for the related complexes. All the complexes were obtained in fair to excellent yields ranging from 60 to 90%. These compounds are air-stable in the solid state and can be stored for months without degradation. In addition, it was possible, for the first time, to structurally characterize the ionic cobalt complexes **6**, **22** and **23** *via* X-ray diffractometry on single crystals.

Molecular structure determinations of **6**, **22** and **23**

Suitable crystals for structure determination were obtained by slowly adding a small excess of diethyl ether into an acetonitrile solution and subsequently cooling down to 2 °C. After 2 days small green crystals for **6**, red-brown crystals for **22** and brown crystals for **23** were formed. The thermal ellipsoid plots

Fig. 1 ORTEP drawings (50% probability) of **6**. For the sake of clarity, hydrogen atoms have been removed and only one cobalt complex is shown.Fig. 2 ORTEP drawings (50% probability) of **23**. For the sake of clarity, hydrogen atoms have been omitted.Fig. 3 ORTEP drawings (50% probability) of **22** showing the two molecules engaged in a hydrogen bond network with 1.5 water molecules.

of **6**, **22** and **23** are shown in Fig. 1–3. The crystallographic data, selected bond lengths and angles of **6**, **22** and **23** are listed in Tables 1–4, respectively.

Table 1 Selected bond lengths (Å) and angles (°) for complex **6** (two discrete complexes present in the independent unit of the elementary cell, only one listed in this table)

Complex 6 /bonds-angles	
Co(2)–N(6)	1.884(2)
Co(2)–N(7)	1.8891(19)
Co(2)–N(8)	1.989(2)
Co(2)–N(5)	2.0011(19)
Co(2)–O(11)	1.9249(17)
Co(2)–O(9)	1.9249(17)
Co(2)···O(10)	3.168
Co(2)···O(12)	3.133
O(7)···H(131)	2.022
N(8)–Co(2)–O(9)	90.55(8)
N(6)–Co(2)–O(9)	88.16(8)
N(7)–Co(2)–O(11)	88.19(8)
N(5)–Co(2)–O(11)	91.21(8)
O(11)–Co(2)–O(9)	175.28(7)
N(7)–Co(2)–N(8)	82.36(8)
N(6)–Co(2)–N(7)	83.96(9)
N(6)–Co(2)–N(5)	81.93(8)
N(8)–Co(2)–N(5)	111.75(8)

All three tetraethyl-ammonium cobalt complexes **6**, **22** and **23** display similar structural patterns including, on the one hand, an octahedral geometry around the negative charged metal center with two monodentate, apical ligands (acetate for **6**, bromo for **22** and **23**) and, on the other hand, the tetradentate N_4 -bpb-ligand occupying the equatorial plane.

Cobalt(III)-bpb anions and the counter-ion, tetraethyl ammonium, display no short contacts as can be representatively seen in the crystal structure of complex **6** $[\text{Co}(\text{bpb}-\text{Cl}_2)-\text{OAc}_2][\text{NEt}_4]$ (Fig. 1).

The molecular structures of compounds **6** and **23** display, in the independent unit of the elementary cell, *two discrete complexes* with water molecules engaged in hydrogen bond networks. For complex **6** the network involves one water molecule and the carbonyl moieties of acetate and amide groups (O(7)–O(13): 2.807 Å; O(13)–O(10): 2.822 Å) whereas in compound **23**, the network includes 1.5 molecules water, one bromide and the carbonyls of two amide groups per independent unit (O(6)–O(5): 2.739 Å; O(3)–O(5): 2.757 Å; O(1)–O(5): 2.816 Å) (Fig. 2). For complex **22** a distinct single complex with no intermolecular short contacts was found in the independent unit of the elementary cell during the structural study (Fig. 3, see ESI† for more details).

Cobalt atoms and the N_4 ligand plane are almost coplanar in the case of the cobalt bromide complexes **22** and **23** (maximal distortion from the mean N_4 -plane: 0.004 Å, distance of Co from the mean planes ranging from 0.005 to 0.007 Å), in the same way as can be noticed in related octahedrally coordinated cobalt porphyrin derivatives.³⁰

In the cobalt acetate complex **6** one independent molecule, involved in the above-mentioned hydrogen bond network, displays coplanar cobalt and N_4 ligand as in **22** and **23** whereas the other one shows a slightly more distorted geometry

Table 2 Crystallographic data for **6**, **22** and **23**

	6 : $2[\text{Co}(\text{bpbCl}_2)\text{OAc}][\text{NEt}_4] \cdot \text{H}_2\text{O}$	22 : $[\text{Co}(\text{bpbNO}_2)\text{Br}_2][\text{NEt}_4]$	23 : $2[\text{Co}(\text{bpbMe}_2)\text{Br}_2][\text{NEt}_4] \cdot 1.5\text{H}_2\text{O}$
Crystal data			
Empirical formula	$\text{C}_{60}\text{H}_{74}\text{Cl}_4\text{Co}_2\text{N}_{10}\text{O}_{13}$	$\text{C}_{26}\text{H}_{31}\text{Br}_2\text{CoN}_6\text{O}_4$	$\text{C}_{56}\text{H}_{75.5}\text{Br}_4\text{Co}_2\text{N}_{10}\text{O}_{5.25}$
Molecular mass	1402.95	710.32	1409.25
Crystal color	Green	Red-brown	Brown
Crystal size (mm ³)	$0.07 \times 0.05 \times 0.04$	$0.147 \times 0.114 \times 0.023$	$0.059 \times 0.049 \times 0.033$
Crystal system	Monoclinic	Monoclinic	Monoclinic
Space group	$P2_1/c$ (no. 14)	$P2_1/c$	$P2_1/c$
<i>a</i> (Å)	21.8010(15)	10.2730(5)	17.8240(15)
<i>b</i> (Å)	15.0617(10)	11.9909(6)	16.6669(14)
<i>c</i> (Å)	21.8954(15)	23.3174(12)	20.3735(17)
α (°)	90	90	90
β (°)	119.0960(10)	101.6220(10)	101.5020(10)
γ (°)	90	90	90
<i>V</i> (Å ³)	6282.3(7)	2813.4(2)	5930.8(9)
<i>Z</i>	8	4	4
<i>D</i> _{calc} (g cm ^{−3})	1.483	1.677	1.578
μ (mm ^{−1})	0.770	3.494	3.310
<i>F</i> (0 0 0)	2920	1432	2866
Wavelength (Å)	0.71073	0.71073	0.71073
<i>T</i> (K)	100(2)	100(2)	100(2)
θ -range (°)	1.72 to 28.49	1.783 to 28.562	1.592 to 28.546
Index ranges	$-28 \leq h \leq 28$, $-20 \leq k \leq 19$, $-28 \leq l \leq 28$	$-13 \leq h \leq 13$, $-15 \leq k \leq 15$, $-30 \leq l \leq 31$	$-23 \leq h \leq 23$, $-21 \leq k \leq 22$, $-27 \leq l \leq 27$
Solution and refinement			
Number of reflections measured	110 733	50 757	106 542
Number of independent reflections	14 943	6730	14 101
GOF	1.019	1.038	1.016
<i>R</i> ₁ [<i>I</i> 2 θ (<i>I</i>)]	0.0423	0.0273	0.0390
<i>wR</i> ₂ [<i>I</i> 2 θ (<i>I</i>)]	0.0888	0.0690	0.0620
Largest <i>e</i> -max, <i>e</i> -min (e Å ^{−3})	0.850 and −0.686	0.846 and −0.518	0.651 and −0.506

Table 3 Selected bond lengths (Å) and angles (°) for complex **22**

Complex 22/bonds-angles	
Co(1)–N(1)	1.8763(17)
Co(1)–N(2)	1.8766(17)
Co(1)–N(3)	1.9772(17)
Co(1)–N(4)	1.9840(17)
Co(1)–Br(1)	2.4143(4)
Co(1)–Br(2)	2.4029(4)
N(2)–Co(1)–Br(2)	90.81(6)
N(4)–Co(1)–Br(2)	89.82(5)
N(3)–Co(1)–Br(1)	89.61(5)
N(1)–Co(1)–Br(1)	90.41(6)
Br(1)–Co(1)–Br(2)	1.78727(15)
N(2)–Co(1)–N(1)	84.50(8)
N(2)–Co(1)–N(3)	82.81(8)
N(3)–Co(1)–N(4)	109.74(7)
N(1)–Co(1)–N(4)	82.95(7)

Table 4 Selected bond lengths (Å) and angles (°) for complex **23** (two discrete complexes present in the independent unit of the elementary cell, only one listed in the table)

Complex 23/bonds-angles	
Co(2)–N(5)	1.975(2)
Co(2)–N(6)	1.878(2)
Co(2)–N(7)	1.882(2)
Co(2)–N(8)	1.990(2)
Co(2)–Br(3)	2.4136(5)
Co(2)–Br(4)	2.4008(5)
N(5)–Co(2)–Br(3)	87.87(7)
N(7)–Co(2)–Br(3)	91.91(8)
N(6)–Co(2)–Br(4)	91.23(7)
N(8)–Co(2)–Br(4)	89.33(7)
Br(3)–Co(2)–Br(4)	175.17(2)
N(5)–Co(2)–N(6)	83.15(10)
N(6)–Co(2)–N(7)	84.33(10)
N(7)–Co(2)–N(8)	82.63(11)
N(8)–Co(2)–N(5)	109.89(10)

(maximal distortion from the mean N_4 -plane: 0.02 Å, distance of Co from the mean planes ranging from 0.042 Å; for more information see ESI†). The bond lengths between cobalt- and nitrogen bpb-atoms found in **6**, **22** and **23** can be divided into “weak” bonds for the pyridine-N-atoms with values ranging

from 1.975(2) (complex **23**) to 2.001(2) (complex **6**) and “strong” bonds for the amide-N-atoms with values from 1.8763(17) (complex **22**) to 1.8886(19) (complex **6**). Considering the N–Co–N angles found in the three complexes, the angles involving the two pyridines are wider than the theoretical value with data ranging from 109.7 to 111.7°, and the other angles fluctuate from 81.9 to 84.5°.

The angles involving cobalt and the two axial monodentate bond ligands (acetate for **6**, bromo for **22** and **23**) are between 175 and 178°, displaying an almost symmetric coordination of the axial ligands. For compound **6** the distances between the axial oxygen atoms and the cobalt atom are Co(2)–O(9): 1.9250(18) and Co(2)–O(11): 1.9249(18), typical for monodentate bound carboxylates (non-coordinated oxygens: Co(2)···O(10): 3.168 and Co(2)–O(12): 3.133). These values are very similar to the data we obtained for the cobalt-acetate complex without substitution at the ligand backbone.¹⁸ The distances between axial bromides and the cobalt atom in compound **22** (Co–Br(1): 2.4143(4) and Co–Br(2): 2.4029(4)) and compound **23** (Co(2)–Br(3): 2.4136(5) and Co(2)–Br(4): 2.4008(5)) are comparable, regardless of the substitution of the ligand linker.

Catalytic screening of the metal bpb complexes in the coupling of epoxides with carbon dioxide

Inspired by the promising results of the screening tests¹⁸ run with the cobalt and iron complexes **5**, **9**, **13** and **20**, we performed similar tests with the new derivatives. The catalytic screening was carried out in 70 ml SS316Ti autoclaves with a standard reaction time of 20 h under “solvent-free” conditions. The results are summarized in Table 5 for the *cobalt-acetate* complexes **5**–**8**, in Table 6 for the different *metal-chloride* complexes **9**–**19** and in Table 7 for the *cobalt-bromide* complexes **20**–**24**. Additionally several commercially available epoxides were examined with one of the efficient catalysts in this range: compound **10** (Table 8). The reaction parameters (cat.%, temp. and P) used in the screening were chosen according to the related literature and quickly checked in a screening with complex **10** and propylene oxide (see ESI†). Last but not least,

Table 5 Coupling reaction with *cobalt-acetate*-complexes^a

Entry	Catalyst	Epoxide	Conversion ^b	Selectivity of the coupling ^c	CO ₃ -content (%) of the polymer ^d	M_n (g mol ^{−1}) ^e	M_w/M_n ^e
1	5 (Co/LH ₂ /OAc)	CHO	64	100/0	100	9600	1.15
2	6 (Co/LCl ₂ /OAc)	CHO	70	100/0	100	7600	1.28
3	7 (Co/LNO ₂ /OAc)	CHO	35	100/0	100	10 100	1.27
4	8 (Co/LMe ₂ /OAc)	CHO	83	100/0	100	8600	1.27
5 ^f	5 (Co/LH ₂ /OAc)	PO	62	0/100			
6	6 (Co/LCl ₂ /OAc)	PO	50	0/100			
7	7 (Co/LNO ₂ /OAc)	PO	32	0/100			
8	8 (Co/LMe ₂ /OAc)	PO	70	0/100			

^a Standard reaction conditions: 10 ml of epoxide, 20 h, 0.5 mol% catalyst, 80 °C, 50 bar for CHO and 35 bar of CO₂ for PO (~7 g CO₂).

^b Conversion = $\eta(\text{monomer units in isolated product})/\eta(\text{epoxide}) \times 100$. ^c Mass of isolated long chain polymers/mass of isolated cyclic monomer.

^d Evaluated *via* ¹H NMR. ^e Evaluated *via* gel permeation chromatography. ^f Ref. 18.

Table 6 Coupling reaction with metal-chloride-complexes^a

Entry	Catalyst	Epoxide	Conversion ^b	Selectivity of the coupling ^c	CO ₃ -content (%) of the polymer ^d	M _n (g mol ⁻¹) ^e	M _w /M _n ^e
1	9 (Co/LH ₂ /Cl ₂)	CHO	67	100/0	100	6500	1.32
2	10 (Co/LCl ₂ /Cl ₂)	CHO	78	100/0	100	8800	1.18
3	11 (Co/LNO ₂ /Cl ₂)	CHO	83	100/0	100	7900	1.33
4	12 Co/LMe ₂ /Cl ₂)	CHO	Traces				
5	13 (Fe/LH ₂ /Cl ₂)	CHO	31	100/0	97	2600	1.14
6	14 (Fe/LCl ₂ /Cl ₂)	CHO	25	100/0	91	2000	1.06
7	15 (Fe/LNO ₂ /Cl ₂)	CHO	27	100/0	100	2700	1.15
8	16 (Fe/LMe ₂ /Cl ₂)	CHO	33	100/0	100–	2200	1.18
9	17 (Cr/LH ₂ /Cl ₂)	CHO	7	100/0	38	600	1.37
10	18 (Cr/LCl ₂ /Cl ₂)	CHO	9	100/0	21	550	1.19
11	19 (Cr/LMe ₂ /Cl ₂)	CHO	Traces	—	—	—	—
12 ^f	9 (Co/LH ₂ /Cl ₂)	PO	76	0/100	—	—	—
13	10 (Co/LCl ₂ /Cl ₂)	PO	86	0/100	—	—	—
14	11 (Co/LNO ₂ /Cl ₂)	PO	92	0/100	—	—	—
15	12 Co/LMe ₂ /Cl ₂)	PO	Traces	—	—	—	—
16 ^f	13 (Fe/LH ₂ /Cl ₂)	PO	78	0/100	—	—	—
17	14 (Fe/LCl ₂ /Cl ₂)	PO	83	0/100	—	—	—
18	15 (Fe/LNO ₂ /Cl ₂)	PO	92	0/100	—	—	—
19	16 (Fe/LMe ₂ /Cl ₂)	PO	91	0/100	—	—	—
20	17 (Cr/LH ₂ /Cl ₂)	PO	90	0/100	—	—	—
21	18 (Cr/LCl ₂ /Cl ₂)	PO	69	0/100	—	—	—
22	19 (Cr/LMe ₂ /Cl ₂)	PO	96	0/100	—	—	—

^a Standard reaction conditions: 10 ml of epoxide, 20 h, 0.5 mol% catalyst, 80 °C, 50 bar for CHO and 35 bar of CO₂ for PO (~7 g CO₂).

^b Conversion = $n(\text{monomer units in isolated product})/n(\text{epoxide}) \times 100$. ^c Mass of isolated long chain polymers/mass of isolated cyclic monomer.

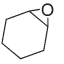
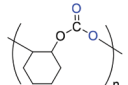
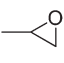
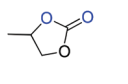
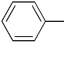
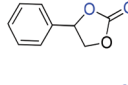
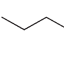
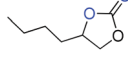
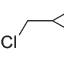
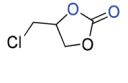
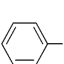
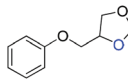
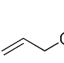
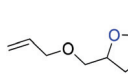
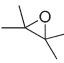
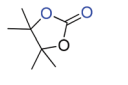
^d Evaluated *via* ¹H NMR. ^e Evaluated *via* gel permeation chromatography. ^f Ref. 18.

Table 7 Coupling reaction (PO/CO₂) with cobalt-bromide-complexes^a

Entry	Catalyst	Catalyst loading (mol%)	Conversion ^b	Selectivity of the coupling ^c
1	20 ^d (Co/LH ₂ /Br ₂)	0.5	93	0/100
2	20 (Co/LH ₂ /Br ₂)	0.1	93	0/100
3	20 (Co/LH ₂ /Br ₂)	0.05	72	0/100
4	21 (Co/LCl ₂ /Br ₂)	0.5	91	0/100
5	21 (Co/LCl ₂ /Br ₂)	0.1	91	0/100
6	21 (Co/LCl ₂ /Br ₂)	0.05	82	0/100
7	22 (Co/LNO ₂ /Br ₂)	0.5	93	0/100
8*	22 (Co/LNO ₂ /Br ₂)	0.1	91	0/100
9**	22 (Co/LNO ₂ /Br ₂)	0.05	76	0/100
10	23 (Co/LMe ₂ /Br ₂)	0.5	93	0/100
11	23 (Co/LMe ₂ /Br ₂)	0.1	75	0/100
12	23 (Co/LMe ₂ /Br ₂)	0.05	64	0/100

^a Standard reaction conditions: 10 ml of epoxide, 20 h, *22 h, **25 h, 80 °C, 35 bar of CO₂ for PO (~7 g CO₂). ^b Conversion = $n(\text{monomer units in isolated product})/n(\text{epoxide}) \times 100$. ^c Mass of isolated long chain polymers/mass of isolated cyclic monomer. ^d Ref. 18.

Table 8 Epoxide-CO₂-coupling reaction catalyzed by 10^a

Entry	Epoxide	Product	p (bar)	Conversion ^b
1			50	76
2			35	78
3			50	60
4			50	60
5			50	96
6			50	93
7			50	99
8			50	0

^a Standard reaction conditions: 10 ml of epoxide, 20 h, 0.2 mol% catalyst, 80 °C. ^b Conversion = $n(\text{monomer units in isolated product})/n(\text{epoxide}) \times 100$.

an exploratory recycle study was accomplished for catalyst 23 using propylene oxide as the substrate (Fig. 4).

In the case of the cobalt-acetate-complexes (Table 5) the results show that cyclohexene oxide yields pure polycarbonates with 100 per cent carbonate linkages and conversions ranging from 35 (entry 3) to 83% (entry 4). For propylene oxide, only the cyclic monomer is formed with yields up to 70% (entry 8). Interestingly the same cobalt(III)/acetate combination with N₂O₂ salen ligand and tetragonal pyramidal coordination geometry yields slightly different results as reported by Coates and

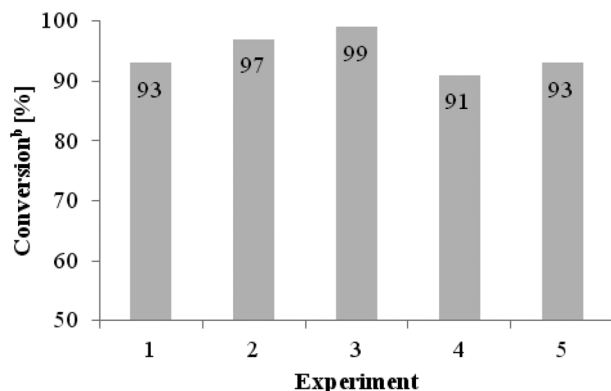


Fig. 4 Recycle experiment with catalyst **23**. Standard reaction conditions: 10 ml of epoxide, 20 h, 0.5 mol% catalyst, 80 °C, 35 bar of CO₂. Conversion = $n(\text{monomer units in isolated product})/n(\text{epoxide}) \times 100$.

co-workers^{12a,b} (polypropylene-carbonate obtained with 30% yield at RT, under *ca.* 54 bar for 2 hours, catalyst: 0.2 mol% and polycyclohexene carbonate obtained with 27% yield, PDI and M_n comparable, run at RT under *ca.* 54 bar, for 20 hours, catalyst: 0.2 mol%). Considering the influence of the bpb-ligand structure on the conversion of the epoxides, a positive effect was found if the aromatic linker was substituted with electron-donating groups (Me) and a negative effect if an electron-withdrawing group (NO₂) was used instead. Only a small influence on the reactivity was noticed with the chlorine substituents probably due to “contradictory” features: on the one hand an electron withdrawing (−I) effect and, on the other hand, a positive mesomeric effect (+M). These results suggest that, for the acetato complexes, the conversion increases with rising electron-donating capability of the ligand: Me > Cl > H > NO₂. Considering now the molecular weight and PDIs of the isolated polymers, ranging from 7600 to 10 100 g mol^{−1} and from 1.15 to 1.28, it seems that the substitution had a fairly small influence on the chain lengths. Generally the gel permeation chromatography elugrams show a bimodal distribution with an overall narrow distribution. This behaviour is most likely due to the presence of water traces in the crystalline compound and the connected formation of cyclohexane-1,2-diol. This behaviour is found in numerous copolymerization reactions producing aliphatic polycarbonates.³¹ All the copolymers isolated with this catalytic system displayed a statistical arrangement of the carbonate linkages (atacticity) as stated by the ¹³C-NMR spectra (CDCl₃, see ESI† for spectra). For instance the copolymer obtained with catalyst **7** displays a strong signal at *ca.* 153.7 ppm for the isotactic and a broad but weaker signal at *ca.* 153.3–153.1 ppm for the syndiotactic fragments.^{32,33}

The cobalt chloride bpb complexes (Table 6, entries 1–4 and 12–15), like the cobalt acetate complexes, form with cyclohexene oxide selectively pure polycarbonates with molecular weights in a narrow range, from 6500 to 8800, and with propylene oxide only the cyclic carbonate. These results can be related to the cobalt-porphyrin-chloride system reported by Sugimoto *et al.* which leads to polycyclohexene carbonate in

99% yield, with higher molecular weights and slightly better PDI (M_n : 14 500 g mol^{−1}, M_w/M_n : 1.13).³⁴ The reaction needed however a cocatalyst like, *e.g.*, 4-dimethylamino-pyridine (reaction conditions: 80 °C, 50 atm pressure CO₂, 0.2 mol% catalyst, 0.1 mol% DMAP, 24 h). Switching the axial ligand from acetate to chloride leads to an increased reactivity with, as an example, a maximal conversion of PO of 92% (Table 6, entry 14) instead of 32% (Table 5, entry 7). This increased reactivity can be related to the presence of the ammonium cation in the ionic complex and an increased reactivity of a concomitantly formed tetraethyl ammonium halide compared to NEt₄OAc (*vide infra* for the mechanism proposal). However the reactivity trend for both epoxides is reversed, the conversion decreasing now with rising electron-donating capability of the ligand: Me < H < Cl < NO₂.

Surprisingly, with complex **12** (entries 4 and 12) only traces of product were found for both epoxides. The solubility test in both epoxides showed that this complex displays a poor solubility in these epoxides which is most likely the explanation for the low catalytic activity.

Taking into account now the catalytic screening of the iron chloride complexes the results reveal that switching the central atom from cobalt to iron has only a small influence on the reactivity towards propylene oxide. A substitution of the aromatic linker has also a general positive effect, leading nearly to the same yields as for the cobalt chloride complexes (*e.g.* entry 18, NO₂-substituted ligand; 92% yield). The effect of the substitution is however not so obvious as in the former case: complex **16** shows, despite containing electron-donating groups, a high activity for propylene oxide, forming cyclic carbonate with 91% yield (entry 19). To put things in perspective, this N₄ bpb-system delivers higher yield of propylene carbonate than the *salan-iron-chloride* system of Rieger and co-workers¹⁵ (57%, at 80 °C, 1 mol% catalyst, 15 bar and 2 hours), and needs however a higher CO₂-pressure and longer reaction time. Changing the test substrate to cyclohexene oxide leads to a lower reactivity with yields reaching only 33 per cent (entry 5) and smaller molecular weights of the isolated copolymer with values from 2000 to 2700 g mol^{−1} compared to the cobalt chloride complexes. Despite a low reactivity, these iron complexes are promising if one considers that most of the reported iron-based molecular catalysts were used in the formation of cyclic carbonates.^{15,35} Our system is however not as efficient as the other homogeneous iron-based copolymerisation catalyst documented by Williams³⁶ and co-workers.

Considering the chromium chloride complexes, the change of the central metal had different influences for propylene- and cyclohexene oxide: On the one hand the conversion is increased up to 96% for propylene oxide (entry 22, Me-substituted ligand) which shows also that, for the chromium chloride complexes, an electron donating group has a positive effect on the conversion. On the other hand, a very low reactivity was found for cyclohexene oxide, with conversions culminating in 9% (entry 10). The incorporation of CO₂ as well as the molecular weights decreased dramatically, with a maximal carbonate linkage value of only 38% (entry 9). Comparing chromium-

cobalt- and iron-bpb-chlorides, a reactivity trend can be roughly established for both epoxides. For propylene oxide all three metals showed high yields with the following gradation of reactivity: $\text{Cr} > \text{Co} \sim \text{Fe}$ whereas for cyclohexene oxide the difference between the metals was more significant and the reactivity trend was as follows: $\text{Co} \gg \text{Fe} > \text{Cr}$.

Unfortunately, it was not possible to enlarge the bpb-metal acetato series and find similar reactivity trends for iron(III)- and chromium(III)-bpb-acetates. The synthesis of the substituted-bpb iron acetates leads surprisingly to low yields while the un-substituted ligand worked properly¹⁸ (90% yield). The maximum yield was reached with the nitro-substituted bpb-iron(III)-acetate (below 30%) that led, in the catalysis, to a very poor conversion to carbonates. The related synthesis with commercially available basic chromium(III) acetate ($[\text{Cr}_3(\mu^3\text{-O})(\text{OAc})_6(\text{H}_2\text{O})_3]\text{Cl}$) led to no conversion whereas freshly made $\text{Cr}(\text{OAc})_2$, with subsequent oxidation, gave complexes in very low yields.

As expected, changing the nature of the axial halide has a significant effect on the catalytic activity. For instance *cobalt bromide bpb* complexes display a very low catalytic activity with cyclohexene oxide, giving only traces of polycyclohexene carbonate. This low reactivity towards cyclohexene oxide is due to a poor solubility of the complexes in the CO_2 -CHO mixture as observed at the end of the test, after having opened the autoclaves (close to no coloration of the reaction mixtures + unchanged catalysts). For comparison, the results of the screening tests run with propylene oxide are listed in Table 7. The substitution of the axial ligands by bromides leads to an increase of the catalytic activity with conversions up to 93% (entry 1), generally higher than those obtained with the cobalt-chloride complexes. The cobalt-bpb-bromide complexes are highly efficient as shown with tests run with a catalyst loading as low as 0.05 mol% (entries 3, 6, 9 and 12). The high efficiency of cobalt bromide complexes is well documented with *e.g.* bromo-cobalt *salen* complexes^{12a} which displayed a high reactivity, producing however polypropylene carbonate in high yields at room temperature. Slight differences in the catalytic activity were found, indicating the positive influence on the reactivity of electron-withdrawing substituents. This behavior was also found for cobalt-bromide complexes newly investigated by Gosh *et al.* with a similar variation of the ligand-backbone.³⁷

Considering more generally the axial ligands/leaving groups present in the cobalt bpb complexes the following reactivity trend could be found for propylene oxide: $\text{Br} > \text{Cl} > \text{OAc}$.

In order to evaluate the limits of these new bpb complexes, we performed a somewhat broader catalytic screening with catalyst **10** using a range of commercially available epoxides. The results of the screening are listed in Table 8, the reactivity trends being for the most part in agreement with the literature.^{9,10} The experiments were performed at 80 °C and a catalyst concentration of 0.2 mol%. The catalyst showed a high catalytic activity with yields up to 99% (entry 7) forming with each tested epoxide, except 2,3-dimethyl-2,3-epoxybutane, an organic carbonate. A copolymer as a single product was

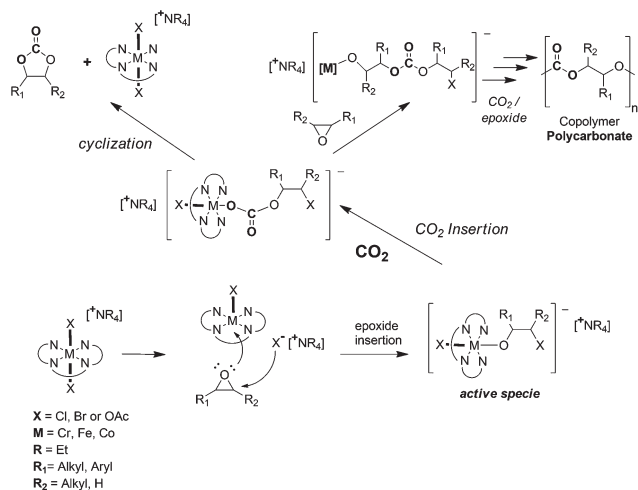
formed merely for cyclohexene oxide (entry 1) whereas for the other epoxides only the cyclic monomers were obtained. The highest yields of cyclic carbonates were attained with mono-substituted epoxides displaying an electron-withdrawing group (entries 5–7) as illustrated by the high conversions reached with glycidyl ethers and epichlorohydrine. This trend was tentatively explained in the literature by the ability of some electron-withdrawing groups to stabilize intermediates and facilitate the intramolecular cyclization.³⁸

Styrene oxide, however, delivered the cyclic carbonate in average yields (entry 3) (see NMR data in ESI†). The somewhat lower reactivity of SO compared to PO and CHO as well as the preferred formation of the cyclic carbonate was already documented in some studies.^{39,40} The reasons depend on the nature of the catalytic system used, involving either inappropriate steric or electronic parameters of the phenyl group or a lower solubility of the catalyst in the styrene oxide- CO_2 mixture. In our case, complex **10** is soluble; the low reactivity of SO with this system is under further study and will be evaluated performing a screening with the other substituted bpb-catalysts.

The presence of substituents on both sides of the epoxide, without a constrained bicyclic structure, is disadvantageous as shown with 2,3-dimethyl-2,3-epoxybutane (entry 8), where no conversion was noticed. Leaving aside purely steric considerations, “monocyclic” poly-substituted epoxides lack the supplementary drive provided by the release of the strain energy contained in a bicyclic structure like, *e.g.*, in cyclohexene oxide, and hence display very low conversions.⁴¹

To evaluate the robustness of the catalyst system, we carried out a typical recycling experiment with PO and catalyst **23** (Fig. 4; reaction conditions: 10 ml of epoxide, 20 h, 0.5 mol% catalyst, 80 °C, 35 bar of CO_2 , five consecutive runs). After the successful conversion of the epoxide, the cyclic carbonate was separated by vacuum distillation and the catalyst directly used for the next cycle. The minimal loss of the catalyst observed during the test was compensated for by adjusting the amount of propylene oxide in order to keep the epoxide-to-catalyst ratio equal (1:200). According to TGA data, catalyst **23** remains stable up to 250 °C. Examination of the re-used catalyst *via* ^1H NMR and IR spectroscopy showed that the catalyst remained unchanged as long as the distillation of propylene carbonate was performed below 150 °C (for TGA of catalyst **23** and spectra see ESI†). These preliminary results are promising and show that *bpb* catalysts can be reused easily without loss of activity in the coupling reaction.

Mechanism proposal, influence of the substituents on reactivity. By varying minimally the structure of the ligand framework with electron-donating or -withdrawing substituents, a perceptible effect on the catalytic activity could be noticed and correlated with the nature of metals and axial ligands used in the complexes. According to numerous mechanisms found in the literature,^{7–12a} a general mechanism matching the findings of the study can be proposed (Fig. 3). The first step in the formation of an organic carbonate involves basically the activation of the epoxide and its ring opening to form a reactive



Scheme 3 Tentative mechanism for a metal-bpb catalysed coupling reaction.

metal-alkoxide, the actual active species in the catalytic cycle. This happens most likely in the case of the ionic bpb complexes with the concomitant help of the “integrated” cocatalyst in the nucleophilic attack on the epoxide. The ammonium cation would play a kind of dual role: on the one hand, in the formation of a coordinative unsaturated complex, able to coordinate/activate the epoxide. On the other hand, the so-formed ammonium halides or -acetate can play a role in a nucleophilic attack on the epoxide.⁴² Although the mechanism depicted in Scheme 3 implies a mono-molecular activation, a mechanism involving two metallic centers, as found in some related *salen* systems, cannot be discarded yet.^{43,44} The second step of the reaction would be the formation of a carbonate linkage *via* the CO_2 insertion into the reactive metal-alkoxide bond. This intermediate can either form a cyclic monomer *via* intramolecular rearrangement or a polycarbonate through further alternating insertions of epoxide and carbon dioxide molecules (the formation of cyclic carbonate *via* backbiting of the copolymer is left aside in the scheme). The nucleophilicity of the “liberated” halide also plays an important role in the opening of the epoxide. The remaining axial ligand might also play a role *via* an effective “*trans* effect”,^{10,12} either in the epoxide coordination/activation step or in influencing the stability of the metal-alkoxide bond.

For the cobalt-halide complexes a positive influence of the electron-withdrawing groups was found in agreement with the work of Ghosh and co-workers,³⁷ which can be likely explained with a better activation of the epoxide, the metal center being “more” electrophilic.

The chromium(III)-chloride-complexes display on the other hand a reverse influence of the substitution, with an increase of the catalytic activity using electron-donating substituents. Without getting deeper into frontier molecular orbital theories and molecular modelling, the “Hard Soft Acid Base” principle⁴⁵ might explain the observed trends (owing to the good solubility of the catalysts, solubility effects depending on the

substituents can be neglected). Chromium(III) can be considered as a Lewis acid (LA) a tad harder than cobalt(III),⁴⁶ while chloride can be seen as a Lewis base (LB) somewhat harder than acetate. The Cr(III)–chloride combination demonstrates a standard “hard acid–hard base” match. Electron-donating substituents would force electrons in the ligand causing the metal acidic center to be “less” hard; this would “destabilize” the chromium chloride complex enhancing its reactivity. A parallel can be drawn to the cobalt(III) acetate complexes which display the same trend, the Co(III)–acetate pair being however a tad softer than the Cr(III)–chloride one. Along these lines, the higher reactivity of the Co(III)–chloride–bpb complexes suggests also that hardness of Co(III) and acetate match better (higher stability of the complex) than in the case of Co(III) and chloride. Considering now the contradicting case of the bpb-cobalt-chloride complexes, the acid–base HSAB match is not as optimal as for the Cr(III)–chloride pair, the Co(III) ion being softer. Electron-withdrawing substituents would cause the metal center to be harder, allowing a more reactive LA–LB match.

Unfortunately in the case of iron(III) a substituent/reactivity correlation is not so apparent, weakening to some extent this LA–LB approach. Both types of substitutions had however a positive effect on the reactivity compared to the “bare” ligand.

Conclusions

We have synthesized new iron, chromium and cobalt complexes displaying ligands with a *N,N*-bis(2-pyridine-carboxamide)-1,2-benzene framework displaying either electron donating- or electron withdrawing substituents. These ionic complexes encompass tetraalkylammonium counter-ions as potential cocatalysts. Some of the new complexes: cobalt/acetate/bpb- Cl_2 complex **6**, cobalt/bromo/bpb- NO_2 complex **22** and cobalt/bromo/bpb- Me_2 **23** could be for the first time structurally characterized *via* X-ray diffraction. The complexes were tested towards the coupling of epoxides and carbon dioxide and compared with the results obtained with the “parent compounds”.¹⁸ The screening showed that some of the ionic catalysts with substituted linkers actually work more efficiently than those with standard linkers, leading in some cases selectively to pure alternating copolymers in the case of cyclohexene oxide and to high amounts of monomeric cyclic carbonate with terminal epoxides (*e.g.* PO). A broader catalytic screening suggests in agreement with the literature that terminal epoxides displaying electron-withdrawing functional groups are favored with this sort of catalysts. In addition a recycling screening indicates that *bpb* catalysts can be reused easily without loss of activity in the coupling reaction. Based on the data gathered in this study, we could also observe some reactivity trends relative to the substituents located at the aromatic linker, the nature of the axial ligand and of the metal and proposed a tentative mechanism.

Acknowledgements

We thank the Helmholtz Research School Energy-Related Catalysis for financial support.

Notes and references

- W. Leitner, *Appl. Organomet. Chem.*, 2000, **14**, 809.
- <http://www.novomer.com>, <http://www.empowermaterials.com/>
- M. Zhang, B. Liu, L. Chen and A. Yu, *Macromol. Rapid Commun.*, 2002, **23**, 881.
- J. H. Clements, *Ind. Eng. Chem. Res.*, 2003, **42**, 663.
- S. Inoue, H. Koinuma and T. Tsuruta, *J. Polym. Sci., Part B: Polym. Lett.*, 1969, **7**, 287.
- S. Inoue, H. Sugimoto and H. Ohtsuka, *J. Polym. Sci., Part A: Polym. Chem.*, 2004, **42**, 5561.
- G. W. Coates and D. R. Moore, *Angew. Chem., Int. Ed.*, 2004, **43**, 2.
- D. J. Darensbourg, *Chem. Rev.*, 2007, **107**, 2388.
- C. K. Williams, M. R. Kember and A. Buchard, *Chem. Commun.*, 2011, **47**, 141.
- P. P. Pescarmona and M. Taherimehr, *Catal. Sci. Technol.*, 2012, **2**, 2169.
- X.-B. Lu, W.-M. Ren and G.-P. Wu, *Acc. Chem. Res.*, 2012, **45**, 1721.
- (a) G. W. Coates, C. T. Cohen and T. Chu, *J. Am. Chem. Soc.*, 2005, **127**, 10869; (b) C. T. Cohen, C. M. Thomas, K. L. Peretti, E. B. Lobkovsky and G. W. Coates, *Dalton Trans.*, 2006, 237.
- S. Inoue and N. Takeda, *Makromol. Chem.*, 1978, **179**, 1377.
- D. J. Darensbourg and S. B. Fitch, *Inorg. Chem.*, 2007, **46**, 5474.
- B. Rieger, J. B. Dengler, M. W. Lehenmeier, S. Klaus, C. E. Anderson and E. Herdtweck, *Eur. J. Inorg. Chem.*, 2011, 336.
- K. D. Janda and T. S. Reger, *J. Am. Chem. Soc.*, 2000, **122**, 6929.
- K. Yu and C. W. Jones, *Organometallics*, 2003, **22**, 2571.
- M. Adolph, T. A. Zevaco, O. Walter, E. Dinjus and M. Döring, *Polyhedron*, 2012, **48**, 92.
- (a) N. Yamazaki and F. Higashi, *Tetrahedron*, 1974, **30**, 1323; (b) R. S. Vagg, D. J. Barnes, R. L. Chapman and E. C. Watton, *J. Chem. Eng. Data*, 1978, **23**, 349.
- R. N. Mukherjee and M. Ray, *Polyhedron*, 1992, **11**, 2929.
- R. N. Mukherjee, M. Ray, J. F. Richardson and R. M. Buchanan, *J. Chem. Soc., Dalton Trans.*, 1993, 2451.
- X.-G. Zhou, J.-L. Zuo, L. Yang, R.-N. Wei and R. Li, *J. Mol. Catal. A: Chem.*, 2007, **266**, 284.
- Y. Kim, Y. W. Choi, S. H. Kim, D. N. Lee and C. Kim, *Acta Cryst. E*, 2006, **62**, m2715.
- Bruker, Bruker AXS Inc., Madison, Wisconsin, USA, 2007; G. M. Sheldrick, *Acta Crystallogr., Sect. A: Fundam. Crystallogr.*, 2008, **64**, 112; L. Zsolnai, XPM, University of Heidelberg, Germany, 1996.
- C. R. Groom and F. H. Allen, *Wiley Interdiscip. Rev.: Comput. Mol. Sci.*, 2011, **1**, 368.
- MERCURY 3.0 (Build RC5); <http://www.ccdc.cam.ac.uk/mercury>
- D. J. Darensbourg, J. L. Rodgers, R. M. Mackiewicz and A. L. Phelps, *Catal. Today*, 2004, **98**, 485.
- D. J. Darensbourg and S. B. Fitch, *Inorg. Chem.*, 2008, **47**, 11868.
- W. Zhang, B. Y. Liu, C.-Y. Tian, L. Zhang and W. Yan, *J. Polym. Sci., Part A: Polym. Chem.*, 2006, **44**, 6243.
- O. Q. Munro, S. C. Shabalala and N. Brown, *Inorg. Chem.*, 2001, **40**, 3303.
- C. K. Williams, F. Jutz, A. Buchard, M. R. Kember and S. B. Fredriksen, *J. Am. Chem. Soc.*, 2011, **133**, 17395.
- K. Nozaki, K. Nakano and T. Hiyama, *Macromolecules*, 2001, **34**, 6325.
- G. W. Coates, M. Cheng, N. A. Darling and E. B. Lobkovsky, *Chem. Commun.*, 2000, 2007.
- K. Kuroda and H. Sugimoto, *Macromolecules*, 2008, **41**, 312.
- M. A. Fuchs, T. A. Zevaco, E. Ember, O. Walter, I. Held, M. Döring and E. Dinjus, *Dalton Trans.*, 2013, **42**, 5322.
- C. K. Williams, A. Buchard, M. R. Kember and K. G. Sandeman, *Chem. Commun.*, 2011, **47**, 212.
- A. Ghosh, P. Ramidi, N. Gerasimchuk, Y. Gartia and C. M. Felton, *Dalton Trans.*, 2013, **42**, 13151.
- G.-P. Wu, S.-H. Wei, W.-M. Ren, X.-B. Lu, T.-Q. Xu and D. J. Darensbourg, *J. Am. Chem. Soc.*, 2011, **133**, 15191.
- G.-P. Wu, S.-H. Wei, W.-M. Ren, X.-B. Lu, B. Li, Y.-P. Zu and D. J. Darensbourg, *Energy Environ. Sci.*, 2011, **4**, 5084.
- N. D. Harrold, Y. Li and M. H. Chisholm, *Macromolecules*, 2013, **46**, 692.
- K. Morokuma, Z. Liu and M. Torrent, *Organometallics*, 2002, **21**, 1056.
- X.-B. Lu, X.-J. Feng and R. He, *Appl. Catal., A*, 2002, **234**, 25.
- X.-B. Lu and D. J. Darensbourg, *Chem. Soc. Rev.*, 2012, **41**, 1462.
- R. L. Paddock and S. T. Nguyen, *J. Am. Chem. Soc.*, 2001, **123**, 11498.
- R. G. Pearson, *J. Chem. Educ.*, 1968, **45**, 581.
- R. G. Pearson, *Inorg. Chem.*, 1988, **27**, 734.